Direct Modeling of the Starting Process of Skewed Rotor Induction Motors Using a Multi-Slice Technique

S. L. Ho W. N. Fu H.C. Wong*

Dept. of Electrical Engineering *Industrial Centre
The Hong Kong Polytechnic University, Hong Kong

***Abstract* - Both the starting current and the starting torque of induction motors cannot be evaluated and measured accurately and readily. In particular, the geometrical features of the skewed rotor bars are very difficult to study if a general 2-D finite element method is used. This paper presents an approach in using a multi-slice, time stepping 2-D eddy-current finite element method to study the starting processes of skewed rotor induction machines. The fields of the multi-slices are being solved *en bloc* simultaneously, and thus the eddy current effects can be taken into account directly. New forms of the governing equations for the multi-slice model are derived so as to allow the meshes of the multi-slices to be taken as one 2-D mesh. The resultant algorithm is then very similar to that of general 2-D problems. Special time stepping techniques for studying the starting process of motors are also presented. The performances of motors with skewed and non-skewed rotor are shown. It was found that the simulation results correlated very well with test data.**

***Index terms* – Induction motors, finite element methods.**

I. INTRODUCTION

The starting current and the starting torque are important quality indexes for induction motors. An accurate evaluation of these quantities is always very challenging. The main reasons for such difficulties are because these parameters are greatly influenced by skin effect in the rotor and saturation in the slot teeth. All these factors are changing dynamically during the starting processes. Even after the prototypes are made, it is sometimes difficult to measure the starting torque readily if the machines are large.

With the advent of computing power and numerical methods in recent years, it has become practical to use finite element methods (FEM) to compute the magnetic fields in electrical machines. Such numerical techniques should enable the designer to solve problems that are difficult to consider by using the analytical approach. Many empirical factors then become unnecessary.

For induction motors with non-skewed rotor bars, a time stepping two dimensional (2-D) FEM which is coupled to the external circuit equations and mechanical equation, has been successfully developed. The method can take into account the skin effect, the machine rotation and the non-sinusoidal quantities in the mathematical models directly [1-2]. However, almost all practical induction motors have skewed rotor bars, and such geometrical feature presents an enormously difficulty if 2-D FEM is used. Note however that compared with the 3-D FEM, the 2-D FEM has the advantages of having simple mesh generation, short computing time and small computer storage. So it would be highly desirable if a 2-D model can be developed to study motors with skewed bars.

One possible technique is to represent a skewed motor with a 2-D multi-slice model [3]. A set of non-skewed 2-D models, each corresponding to a section taken at different positions along the axis of the machine, is used to model the skewed rotor. In order to ensure that the current flowing in the bars of one slice is the same as that flowing in the bars of every other slices of the same rotor bar, it will be necessary to carry out the field solutions simultaneously for all slices. Piriou et al. [4] has used this method to simulate a permanent magnet synchronous machine. However the eddy current in the model was not considered. Gyselinck et al. [5] also used the multi-slice method to simulate the steady-state operation of a squirrel cage induction motor. The system equations were separated into several sub-groups [5]. The disadvantage of such method is the need for the sub-systems of the equations to have identical solutions with that of the original system of equations. However the coefficient matrixes of the system equations are non-linear and the solutions of the sub-system of equations will affect each other. Thus the solutions may not always converge rapidly. Boualem et at. [6] also used the multi-slice approach to simulate the operation of a squirrel cage induction motor, although the end ring inductance was not considered. In those studies reported [4-6], the magnetic equations on each slice were separately established and then coupled together before such equations are being solved. This will introduce unnecessary complexities in the software programs.

Alternatively, one can use circuit models instead of eddy-current models in which the slice models may be solved — independently, rather than simultaneously. The disadvantage is that the eddy-current effect is not included

PE-I190-EC-0-2-1998 A paper recommended and approved by the IEEE Electric Machinery Committee of the IEEE Power Engineering Society for publication in the IEEE Transactions on Energy Conversion. Manuscript submitted August 27, 1997; made available for printing February 18, 1998.

in the field solution [7]. That is to say, the skin effect, which is especially important during the starting process, cannot be taken into account directly.

In this paper new forms of governing equations for models with coupled multi-slices are derived. Program of the single slice model can be easily extended to deal with the multi-slice model from the equations derived. The divisions of the slices in the axial length can also be non-uniform. Special techniques needed in the time stepping for starting process of motors is also described. The developed program can be run on personal computers. With the proposed method, the skewing effect, the skin effect, saturation, rotor movement and the non-sinusoidal quantities can all be included directly in the system equations. When the applied terminal voltage is known, the currents, torque, etc., can be computed directly. The performances of motors with skewed and non-skewed rotor can be studied. The test results of two identical 11 kW skewed cage induction motors are used to verify the computed results.

II. BASIC EQUATIONS OF MULTI-SLICE MODEL

The following assumptions are made:

1. There are no leakage fluxes in the outer surface of the stator core and in the inner surface of the rotor core.

2. As the iron cores are laminated, the eddy currents in the iron cores are neglected in the mathematical model.

3. The end effects are considered by coupling the electrical circuits into the FEM equations. The leakage inductances at the end of the stator windings and at the end rings of the rotor cage are obtained by analytical methods.

4. The motor in the axial direction is considered as composing of multi-slices. In each slice the magnetic vector potential has an axial component only. The magnetic field is present in planes normal to the machine axis. Hence the characteristics of the electromagnetic field of each slice is two-dimensional. The relationship between slices is based on the principle that the current flowing in the bars of one slice is the same as that which flows in the same bars of every other slices.

According to the stated assumptions, the Maxwell's equations applied to all domains under investigation will give rise to the following equation:

$$\frac{\partial}{\partial x}\left(\upsilon\frac{\partial A}{\partial x}\right)+\frac{\partial}{\partial y}\left(\upsilon\frac{\partial A}{\partial y}\right)=-j \tag{1}$$

A. In the Air-gap and in the Iron Domains

$$j=0 \tag{2}$$

B. In the Rotor Conductor Domain

Because the induced electric field intensity in the k^{th} slice is $-\frac{\partial A^{(k)}}{\partial t}$, the induced electromotive force between the two ends of the conductor being considered is:

$$e^{(k)}=-l^{(k)}\frac{\partial A^{(k)}}{\partial t} \tag{3}$$

where $l^{(k)}$ is the axial length of the k^{th} slice. Using the reference direction as shown in Fig. 1, the total current density $j^{(k)}$ in the conductor of the k^{th} slice is:

$$j^{(k)}=\frac{\sigma}{l^{(k)}}\left(-u^{(k)}+e^{(k)}\right)=-\frac{\sigma}{l^{(k)}}\left(u^{(k)}+l^{(k)}\frac{\partial A^{(k)}}{\partial t}\right) \tag{4}$$

where $u^{(k)}$ is the potential difference between the two ends of a conductor in the k^{th} slice and σ is the conductivity of the material. In equation (4) $\frac{\sigma}{l^{(k)}}e^{(k)}$ is the induced eddy current density.

Integrating the current density $j^{(k)}$ over the cross-section of the rotor bar gives:

$$i^{(k)}=-\frac{\sigma}{l^{(k)}}\left(Su^{(k)}+\iint_{\Omega^{(k)}}l^{(k)}\frac{\partial A^{(k)}}{\partial t}\mathrm{d}\Omega\right) \tag{5}$$

where $i^{(k)}$ is the total current in the conductor. $S=\iint_{\Omega^{(k)}}\mathrm{d}\Omega$ is the cross-sectional area of one rotor bar.

By moving $l^{(k)}$ in equation (5) to the left hand side, letting k=1,2,...,M (M is the total number of slices) and grouping all these M equations together, one has

$$\sum_{m=1}^{M}l^{(m)}i^{(m)}=-\sigma\left(S\sum_{m=1}^{M}u^{(m)}+\sum_{m=1}^{M}\iint_{\Omega^{(m)}}l^{(m)}\frac{\partial A^{(m)}}{\partial t}\mathrm{d}\Omega\right) \tag{6}$$

According to assumption 4 the rotor bar current is:

$$i=i^{(1)}=i^{(2)}=\cdots=i^{(M)} \tag{7}$$

Replace $i^{(m)}$ in equation (6) with i, one obtains:

$$i=-\frac{\sigma}{l}\left(Su+\sum_{m=1}^{M}\iint_{\Omega^{(m)}}l^{(m)}\frac{\partial A^{(m)}}{\partial t}\mathrm{d}\Omega\right) \tag{8}$$

where $l=\sum_{m=1}^{M}l^{(m)}$ is the total axial length of the bar and $u=\sum_{m=1}^{M}u^{(m)}$ is the potential differences between the two ends of a bar.

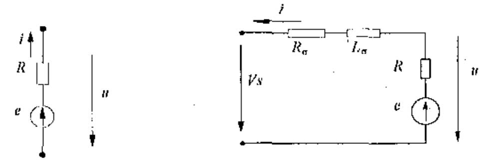

(a) A rotor bar (b) A stator phase circuit

Fig. 1 The reference directions in rotor and stator

Because the items on the right hand side of equation (5) and (8) are equal, one has

$$u^{(k)}=\frac{l^{(k)}}{l}u+\frac{l^{(k)}}{lS}\sum_{m=1}^{M}\iint_{\Omega^{(m)}}l^{(m)}\frac{\partial A^{(m)}}{\partial t}\mathrm{d}\Omega-\frac{1}{S}\iint_{\Omega^{(k)}}l^{(k)}\frac{\partial A^{(k)}}{\partial t}\mathrm{d}\Omega \tag{9}$$

Substituting (9) into (4), one has

$$j^{(k)} = -\left(\frac{\sigma}{l}u + \sigma\frac{\partial A^{(k)}}{\partial t} + \frac{\sigma}{lS}\sum_{m=1}^{M}\iint_{\Omega^{(m)}} l^{(m)}\frac{\partial A^{(m)}}{\partial t}\mathrm{d}\Omega - \frac{\sigma}{S}\iint_{\Omega^{(k)}}\frac{\partial A^{(k)}}{\partial t}\mathrm{d}\Omega\right) \quad (10)$$

Since (10) is applicable to the rotor bars of all slices, the superscript k can be omitted. By substituting (10) into (1), one obtains the basic electromagnetic field equation in the rotor conductor domain as:

$$\frac{\partial}{\partial x}\left(\upsilon\frac{\partial A}{\partial x}\right) + \frac{\partial}{\partial y}\left(\upsilon\frac{\partial A}{\partial y}\right) =$$

$$\frac{\sigma}{l}u + \sigma\frac{\partial A}{\partial t} + \frac{\sigma}{lS}\sum_{m=1}^{M}\iint_{\Omega^{(m)}} l^{(m)}\frac{\partial A^{(m)}}{\partial t}\mathrm{d}\Omega - \frac{\sigma}{S}\iint_{\Omega}\frac{\partial A}{\partial t}\mathrm{d}\Omega \quad (11)$$

Another relationship between i and u can be obtained from the circuit equations for the rotor end windings. Derivation of the circuit equations in the end winding of a rotor is described in [1]. The unknown potential difference u can then be eliminated at first. Equations (8), (11) and the end winding circuit equations will give rise to the governing formulas in the rotor bar domain.

Assume all the slices are grouped together to form one single master slice with the nodes and elements of the FEM mesh being numbered slice by slice sequentially. That is to say, each mesh of the multi-slices are considered as part of one mesh. The data structure of the resulting FEM mesh then becomes the same as that for a general 2-D problem. With (8), the form of the formula is indeed the same as that for a single slice model. With (11), the only differences of the proposed method compared with the single slice model are the last two items on the right-hand side. The integrals of these two items in (11) can however be realized easily in the program by summations using the Newton-Cotes quadrature as described in [8].

C. *In the Stator Conductor Domain*

Because the stator winding generally consists of fine wires, the current density j in the stator conductor is assumed uniform. The stator circuit of one phase is shown in Fig. 1. In keeping with the rotor equations, the reference direction of the stator phase current i is identical with that of the electromotive force.

Assuming the stator winding of one phase consists of w turns in series, the cross-sectional areas of each conductor at one side of the coils are $S_1, S_2,\ldots,S_w$. The area of each conductor at the other side of the coils are S_{w+1}, S_{w+2}, ..., S_{2w}. The total cross-sectional area of one turn at one side of the coil is equal to S. The circuit equations are:

$$V_s = u - R_\sigma i - L_\sigma\frac{\mathrm{d}i}{\mathrm{d}t} \quad (12)$$

$$u = e - Ri \quad (13)$$

where V_s is the applied voltage; i is phase current; R_σ and L_σ are resistance and inductance at the end of winding, respectively; u is the total potential difference of each element in the stator winding; R is the resistance of each element in the stator. The total induced electromotive force in one phase is therefore

$$e = -\frac{1}{S}\sum_{m=1}^{M} l^{(m)}\left[\iint_{S_1^{(m)}}\frac{\partial A^{(m)}}{\partial t}\mathrm{d}\Omega + \iint_{S_2^{(m)}}\frac{\partial A^{(m)}}{\partial t}\mathrm{d}\Omega + \cdots + \iint_{S_w^{(m)}}\frac{\partial A^{(m)}}{\partial t}\mathrm{d}\Omega - \left(\iint_{S_{w+1}^{(m)}}\frac{\partial A^{(m)}}{\partial t}\mathrm{d}\Omega + \iint_{S_{w+2}^{(m)}}\frac{\partial A^{(m)}}{\partial t}\mathrm{d}\Omega + \cdots + \iint_{S_{2w}^{(m)}}\frac{\partial A^{(m)}}{\partial t}\mathrm{d}\Omega\right)\right]$$

$$= -\frac{1}{S}\sum_{m=1}^{M} l^{(m)}\left(\iint_{\Omega_+^{(m)}}\frac{\partial A^{(m)}}{\partial t}\mathrm{d}\Omega - \iint_{\Omega_-^{(m)}}\frac{\partial A^{(m)}}{\partial t}\mathrm{d}\Omega\right) \quad (14)$$

where $\Omega_+^{(m)} = S_1^{(m)} + S_2^{(m)} + \cdots + S_w^{(m)}$ and $\Omega_-^{(m)} = S_{w+1}^{(m)} + S_{w+2}^{(m)} + \cdots + S_{2w}^{(m)}$; Substituting equation (14) into (13), and noting that $R = \frac{2wl}{\sigma S}$ and the total conductor area of one phase is $\Omega^{(m)} = \Omega_+^{(m)} + \Omega_-^{(m)} = 2wS$, one obtains

$$i = -\frac{\sigma}{2wl}\left[Su + \sum_{m=1}^{M} l^{(m)}\left(\iint_{\Omega_+^{(m)}}\frac{\partial A^{(m)}}{\partial t}\mathrm{d}\Omega - \iint_{\Omega_-^{(m)}}\frac{\partial A^{(m)}}{\partial t}\mathrm{d}\Omega\right)\right] \quad (15)$$

Substituting equation (12) into (15), one has

$$i = -\frac{\sigma}{2wl}\left[S\left(V_s + R_\sigma i + L_\sigma\frac{\mathrm{d}i}{\mathrm{d}t}\right) + \sum_{m=1}^{M} l^{(m)}\left(\iint_{\Omega_+^{(m)}}\frac{\partial A^{(m)}}{\partial t}\mathrm{d}\Omega - \iint_{\Omega_-^{(m)}}\frac{\partial A^{(m)}}{\partial t}\mathrm{d}\Omega\right)\right] \quad (16)$$

Equations (1) and (16) constitute the governing formulas in the stator conductor domain. j in (1) can be replaced by $j = i/S$. It is noted that with the data structure described beforehand, the forms of (1) and (16) are the same as that for the single slice model.

If one divides the slice uniformly in the axial length, i.e. $l^{(1)} = l^{(2)} = \cdots = l^{(M)} = l/M$ in equations (8), (11), and (16), $\frac{1}{l}\sum_{m=1}^{M} l^{(m)}\frac{\partial A^{(m)}}{\partial t}$ can be simplified as $\frac{1}{M}\sum_{m=1}^{M}\frac{\partial A^{(m)}}{\partial t}$. By using finite element formulation and coupling the electromagnetic field equations together with the electrical circuit equations, one obtains the following large non-linear system of equations:

$$\begin{bmatrix} K & C \end{bmatrix}\begin{bmatrix} A \\ i \end{bmatrix} + \begin{bmatrix} Q & R \end{bmatrix}\begin{bmatrix} \frac{\partial A}{\partial t} \\ \frac{\partial i}{\partial t} \end{bmatrix} = [P] \quad (17)$$

where the unknowns $[A]$ and $[i]$ are, respectively, the magnetic vector potentials and currents that are required to be evaluated; $[K]$, $[C]$, $[Q]$, $[R]$ are the coefficient matrices and $[P]$ is the vector associated with input voltages.

In simulating the starting process, the following mechanical equation of the motor is also required to be coupled to the FEM model :

$$J_m \frac{d^2\theta}{dt^2} = T_e - T_f = T \tag{18}$$

where J_m is the moment of inertia; θ is the angular position of the rotor; T_e is the electromagnetic torque and T_f is the load torque. The Maxwell Stress Tensor is used in the computation of the electromagnetic torque.

III. GENERATION OF THE FEM MESH

The mesh generation should be simple, robust, and the mesh of the rotor should be allowed to rotate easily. A method to generate meshes for this multi-slice technique will also be presented in this paper. It has been found that the computing time can be reduced substantially. The proposed method consists of the following steps:

A. Generation of the Basic Mesh

Basic meshes at the cross-section of the induction motor being studied is generated at first. In the air gap, the solution domain is divided into two parts: the stator domain and the rotor domain, with each including a part of the air gap. Meshes of the two domains are then generated separately. For each part, the mesh is automatically generated fully using the deduction of points algorithm and the mesh refinement method [9].

B. Rotation of the Mesh

The unknowns at the inner-most nodes of the stator and at the outer-most nodes of the rotor are connected by virtue of the "periodic boundary conditions". That is to say, when the rotor is rotated, the shape of the rotor mesh will not be changed, but the coordinates and the periodic boundary conditions will. Thus the stator mesh and the rotor mesh are required to be generated once and once only.

C. Generation of the Meshes at Other Slices

The geometrical difference between the basic slice and the other slice is that the rotor of the other slice has rotated by a small angle because of the skewing in the rotor bars. The meshes at the other slices can be easily obtained by rotating the basic rotor mesh marginally.

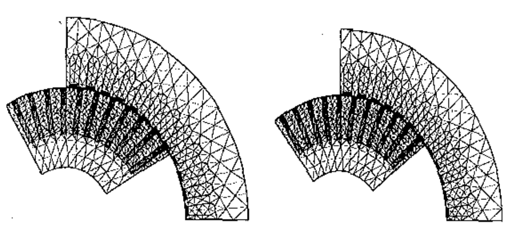

(a) At the first slice (b) At the fourth slice

Fig. 2 FEM meshes of 11 kW skewed motor after a rotation of 30° (4 slices, each has 2523 nodes, 4439 elements) when skin effect needs to be considered

D. Connection of Slices

The nodes, elements, etc. in the FEM model are renumbered slice by slice continually. Therefore, the data structure is two-dimensional. The time stepping FEM is very similar to the general method with the exception of the relationship between the adjacent slices which are introduced in this multi-slice technique. Fig. 2 shows FEM meshes of an 11 kW skewed motor. In rotor to consider the eddy-current during the starting process, a dense mesh is used for the rotor bars. If the speed of the motor is near the synchronous speed, in which the skewed effect can be neglected, the meshes in Fig. 3 are used.

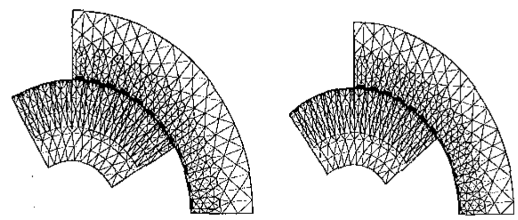

(a) At the first slice (b) At the fourth slice

Fig. 3 FEM meshes of 11 kW skewed motor after a rotation of 30° (4 slices, each has 1626 nodes, 2655 elements) when skin effect does not need to be considered

IV. SOLUTION OF THE SYSTEM OF EQUATIONS

The Backward Euler's method is used to discretize the time variable. If the solution at the $(k\text{-}1)^{th}$ step is known, then at the k^{th} step one has :

$$\omega_k = \omega_{k-1} + \frac{T_k}{J_m}\Delta t \tag{19}$$

$$\theta_k = \theta_{k-1} + \omega_k \Delta t \tag{20}$$

$$\begin{bmatrix} K_k + \dfrac{Q_k}{\Delta t} & C_k + \dfrac{R_k}{\Delta t} \end{bmatrix} \begin{bmatrix} A_k \\ i_k \end{bmatrix} = \begin{bmatrix} \dfrac{Q_k}{\Delta t} & \dfrac{R_k}{\Delta t} \end{bmatrix} \begin{bmatrix} A_{k-1} \\ i_{k-1} \end{bmatrix} + [P_k] \tag{21}$$

where ω is the rotor speed. The rotor FEM mesh is moved in accordance to the rotor movement. The position of the rotor mesh is determined by θ_k. $[K_k]$, $[C_k]$, $[Q_k]$, $[R_k]$ will change with the rotation of the rotor mesh. In the iteration process for solving the equation coupling (19), (20) and (21), the rotor mesh will be changed again and again. This will certainly give rise to difficulties in the program.

The proposed method is, instead of using (19), one could use the Euler's method to obtain an initial gauss of ω_k as follows :

$$\omega_k^{(0)} = \omega_{k-1} + \frac{T_{k-1}}{J_m}\Delta t \tag{22}$$

During the process in solving (21), the rotor mesh is fixed. After the solution of (21) one can then obtain T_k, ω_k can be computed subsequently by using the Backward Euler's method according to (19). The difference between $\omega_k^{(0)}$ and ω_k indicates the discretization error which is dependent on the step size Δt [10]. If this error is larger than that allowed, the step size Δt will be reduced automatically.

At each step of the time stepping process, an iterative solver is most suitable in solving the system of large equations. This is because of the good initial value, which was obtained easily from the result of the last step, has been used to reduce the number of iterations. In this paper the Newton-Raphson method coupled with the incomplete Cholesky-conjugate gradient algorithm are used to solve the system of large non-linear equations.

V. RESULTS

The presented method has been used to simulate the starting operation of two identical 11 kW, skewed rotor cage induction motors (380 V, 50 Hz, Δ connected, 4 poles, 48 slots in stator, 44 slots in rotor, and a skewing of 1.3 stator slot pitch).

The programs are run on a personal computer Pentium / 150 MHz. The motor in the axial direction is divided into 4 slices. For the meshes in Fig. 2, the system equation at each time step has a total of 8962 unknowns. Its solution requires 0.82 min. of CPU time by using the Newton-Raphson method coupled with ICCG method. For the meshes in Fig. 3, the equation has 5394 unknowns. Its solution requires 0.38 min. of CPU time. The basic size of each time step is 0.039 ms. The simulation for the locked rotor test and for the starting process needs a CPU time of about 14 hours and 45 hours, respectively.

The comparison of the results between the computed and experimental data for locked rotor operation at steady state is shown in Table I. Fig. 4 shows the performances of the electromagnetic torques for motors with skewed and non-skewed rotors. Because the torque of skewed motors can be considered as the sum of the torques of many non-skewed motors which are in different relative positions, the torque ripple is relatively smaller in skewed rotor motors compared to their unskewed rotor counterparts. The position of the rotor for the locked rotor test was the same as that given in Fig. 2 except that the rotor has not moved.

For the starting process at no-load conditions, the computed stator phase current is shown in Fig. 5, while the measured values are shown in Fig. 6. The results computed using the proposed method show very good correlation with the test data. The computed electromagnetic torques are shown in Fig. 7 and Fig. 8. It can be noticed that the motors with appropriate skewed rotor bars develops more stable torque than that of non-skewed rotor motor. The high ripple torque may be caused by the relative movement of slots and teeth. A limited number of slices used in the program (to skewed motors) or even a limited number of elements in each one of the slices may also cause such ripple. The precise explanation will however need to be studied further.

The computed magnetic flux distributions at different states of operations are shown in Fig. 9.

TABLE I
COMPARISON OF CURRENTS AND TORQUES AT THE LOCKED ROTOR

	Phase current (RAM)	Torque (Average)
Computed result	148.2 A	145.3 Nm
Test result of motor I	150.4 A	158.4 Nm
Test result of motor II	149.5 A	155.8 Nm

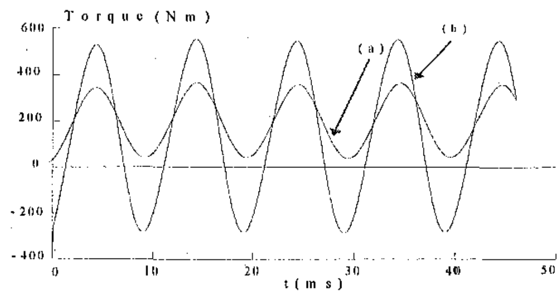

Fig. 4 Computed torque at locked rotor conditions for motor with (a) a skewing of 1.3 stator slot pitch in rotor and (b) unskewed rotor

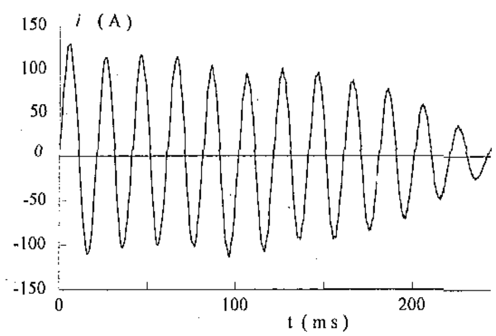

Fig. 5 Computed stator current at the starting process (skewed motor)

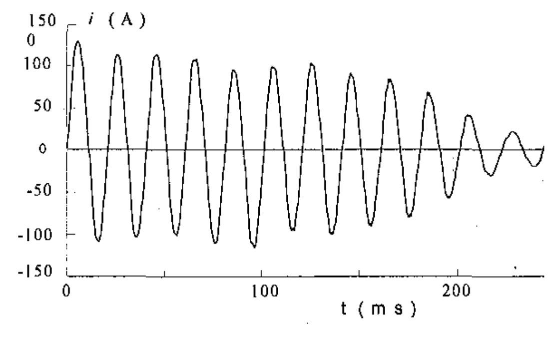

Fig. 6 Measured stator current at the starting process (skewed motor)

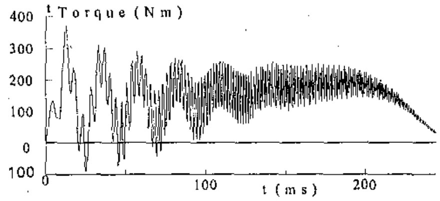

Fig. 7 Computed torque at the starting process (skewed motor)

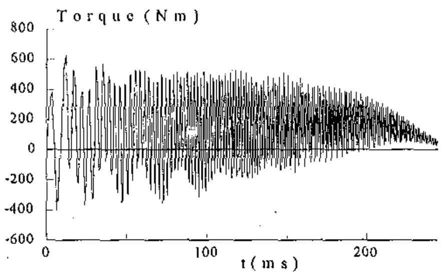

Fig. 8 Computed torque at the starting process (non-skewed motor)

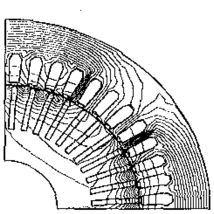

(a) at locked rotor (steady state)

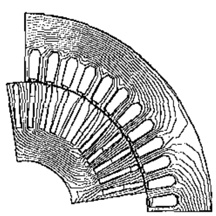

(b) at on load (steady-state)

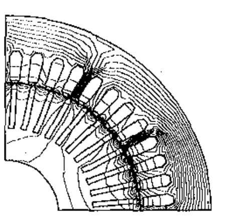

(c) during starting process (t=0.800 ms)

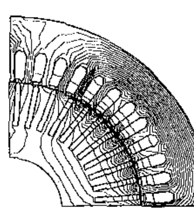

(d) during starting process (t=4.609 ms)

Fig. 9 Computed flux distributions

VI. Conclusion

The skewed geometry of the rotor bars in induction motors has great influences upon the performances of the machines. The proposed multi-slice time stepping 2-D FEM model for skewed motors, with the governing equations similar to that for a general 2-D problem, can be used to precisely simulate the locked rotor operation and the starting process of induction motors. The proposed method solves the fields of multi-slices *en bloc* simultaneously, so the effects of skewed rotor bars, the saturation and the eddy current can all be included in the mathematical model. The method overcomes the difficulties of estimating the starting current and starting torque when using traditional magnetic circuit method and will be applied in the design of machines.

VII. References

[1] A.Arkkio, "Analysis of induction motors based on the numerical solution of the magnetic field and circuit equations", *Helsinki, Acta Polytech. Scandinavica, Elect. Eng'g.,+ Series*, no.59, pp.3-97, 1987.

[2] S.L.Ho and W.N.Fu, "Computation of Harmonic Stray Losses of Induction Motors Using Adaptive Time Stepping Finite Element Method Coupled with Circuits", *Seventh Inter. Conf. on Electrical Machines and Drives*, Conf. Publ. No. 412, Sept., pp. 93-97, 1995.

[3] S.Williamson, "Induction Motor Modelling Using Finite Elements," *Intl. Conf. on Electrical Machines*, France, 5-8 Sept., pp.1-8, 1994.

[4] F.Piriou and A.Razek, "A Model for Coupled Magnetic-Electric Circuits in Electric Machines with Skewed Slots", *IEEE Trans. Magn.* vol. 26, no. 2, pp. 1096-1100, March 1990.

[5] J.J.C.Gyselinck and J.A.A.Melkebeek, "Modelling of Electric Machines with Skewed Slots Using the Two Dimensional Finite Element Method: An Efficient Solving Technique", *Systems Analysis Modelling Simulation*, vol. 18-19, pp. 559-562, 1995,.

[6] B.Boualem and F.Piriou, "Modelling of Induction Motor Accounting for Skewed Slots Effects", *Inter. Conf. on Electrical Machines*, Paris, France, 5-8 Sept., pp. 699-704, 1994.

[7] S.Williamson, Timothy J. Flack and Albertus F. Volschenk, "Representation of Skew in Time-Stepped Two-Dimensional Finite-Element Models of Electrical Machines," *IEEE Industrial Applications Society Annual Meeting*, Colorado, October, 1994.

[8] A.Konrad, "Integrodifferential Finite Element Formulation of Two-Dimensional Steady-State Skin Effect Problems", *IEEE Trans. Magn.*, vol. 18, no. 1, January, pp. 284-292, 1982.

[9] S.L.Ho and W.N.Fu, "A Fully Automatic Mesh Generation Method for the Movement Field Modelling", *The Second Chinese Inter. Conf. on Electrical Machines*, Hangzhou, China, 31 Aug. - 2 Sept., pp. 624-630, 1995.

[10] S.L.Ho, W.N.Fu and H.C.Wong, "Application of Automatic Choice of Step Size for Time Stepping Finite Element Method to Induction Motors", *IEEE Trans. Magn.*, vol. 33, no. 2, March, pp. 1370-1373, 1997.

VIII. Biographies

S. L. Ho was born in 1953. He obtained his BSc and PhD in Electrical Engineering from the University of Warwick, U.K. in 1976 and 1979, respectively. He is currently a member of both the Institution of Electrical Engineers of the U.K. and the Hong Kong Institution of Engineers. He is at present an Associate Professor in the Department of Electrical Engineering, the Hong Kong Polytechnic University. He is the holder of several patents and he has published over 60 papers in journals and in leading conferences. His main research interests also include application of finite elements in electrical machines, phantom loading of machines as well as in the design and development of novel machines.

W. N. Fu was born in 1961 in Zhejiang, China. He received the B.Eng and M.Eng in electrical engineering from Hefei University of Technology and Shanghai University of Technology in 1982 and 1989, respectively. After graduation, he joined the Shanghai University as a lecturer. Since 1994, he has been a visiting scholar at the Hong Kong Polytechnic University. He is now a PhD student. He has published over 35 papers in journals and international conferences. His research interests include electromagnetic field computation and studies on novel machines.

Wong H.C. is the Director of the Industrial Centre at the Hong Kong Polytechnic University. He received his MSc degree from the University of Hong Kong and his DEng from the Xian Jiaotung University, China. He is a fellow of the Institution of Electrical Engineers and the Hong Kong Institution of Engineers. His research interests are in electromagnetic field computation and development of novel machines.